tributed to one dinuclear moiety, appearing at temperature below 20 K. This is one of the lowest temperatures at which EPR spectra of excitonic systems have been observed,[7-9] and a complete single-crystal EPR study of **1** and **2** is being performed and will be reported later.

The magnetic behavior of **2** has been nicely reproduced by considering the magnetism arising from a Heisenberg alternating linear chain plus a Curie paramagnetism from the copper(II) complex. Any interaction between the copper(II) ions and the $TCNQ^-$ ions seems to be too small to be observed with magnetic susceptibility techniques.

Registry No. **1**, 119638-22-1; **2**, 51141-11-8; Zn, 14912-36-8; Cu, 36502-34-8.

Supplementary Material Available: Complete crystallographic data and data collection details for $Zn(phen)_3(TCNQ)_2$ and $Cu(phen)_3(TCNQ)_2$ (Table SI), thermal parameters for $Zn(phen)_3(TCNQ)_2$ (Table SII) and $Cu(phen_3)(TCNQ)_2$ (Table SIII), and positional parameters of the hydrogen atoms of $Zn(phen)_3(TCNQ)_2$ (Table SIV) and $Cu(phen)_3(TCNQ)_2$ (Table SV) (7 pages); listings of the observed and calculated structure factors for $Zn(phen)_3(TCNQ)_2$ (Table SVI) and $Cu(phen)_3(TCNQ)_2$ (Table SVII) (32 pages). Ordering information is given on any current masthead page.

Contribution from the Department of Chemistry, University of Florence, Florence, Italy, and Laboratoire de Chimie (UA CNRS 1194), Department de Recherche Fondamentale, Centre d'Etudes Nucleaires de Grenoble, Grenoble, France

Synthesis, X-ray Crystal Structure, and Magnetic Properties of Two Dinuclear Manganese(II) Compounds Containing Nitronyl Nitroxides, Imino Nitroxides, and Their Reduced Derivatives

A. Caneschi,[1a] D. Gatteschi,*[,1a] J. Laugier,[1b] P. Rey,*[,1b] and C. Zanchini[1a]

Received October 5, 1988

The nitronyl nitroxide 2-phenyl-4,4,5,5-tetramethyl-4,5-dihydro-1*H*-imidazolyl-1-oxy 3-oxide (NITPh) is reduced in the reaction with manganese(II) hexafluoroacetylacetonate ($Mn(hfac)_2$) to yield 1-hydroxy-2-phenyl-4,4,5,5-tetramethyl-4,5-dihydro-1*H*-imidazole (IMHPh). A solid compound of formula $[Mn(hfac)_2(IMHPh)]_2(NITPh)$ (I) is obtained, whose crystal structure was determined through X-ray diffraction. I crystallizes in the triclinic $P\bar{1}$ space group: a = 13.566 (2) Å, b = 15.079 (3) Å, c = 21.622 (4) Å, α = 68.36 (2)°, β = 77.18 (2)°, γ = 61.47 (2)°, Z = 2. A similar behavior was observed with the imino nitroxide 2-phenyl-4,4,5,5-tetramethyl-4,5-dihydro-1*H*-imidazolyl-1-oxy (IMPh) and $Mn(hfac)_2{\cdot}2H_2O$. In this case a solid compound of formula $Mn(hfac)_2(IMHPh)(IMPh)$ (II) is obtained, which crystallizes in the monoclinic space group $P2_1/c$: a = 13.391 (2) Å, b = 22.725 (3) Å, c = 14.987 (2) Å, β = 66.73 (2)°, Z = 4. The crystal structure of I consists of two different centrosymmetric units, of formulas $[Mn(hfac)_2(IMHPh)(NITPh)]_2$ and $[Mn(hfac)_2(IMHPh)]_2$, respectively. The reduced form of the radical bridges the manganese(II) ions in both units, and in the former, a molecule of radical is hydrogen bonded to its reduced form. The crystal structure of II consists of centrosymmetric units $[Mn(hfac)_2(IMHPh)(IMPh)]_2$ with a geometry similar to that of the corresponding unit of I. The magnetic properties of both I and II were studied in the range 5–300 K, showing that the manganese ions are weakly coupled in an antiferromagnetic fashion. The EPR spectra were attributed to the coupled S = 5 state.

Introduction

Nitronyl nitroxides, of the general formula

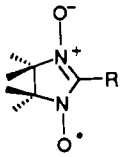

which we abbreviate as NITR, R being phenyl, methyl, ethyl, etc., display a very interesting coordination chemistry with transition-metal ions.[2-4] In fact, it has been found that they can bind in several different ways, with one oxygen atom to one metal ion, yielding discrete mononuclear complexes[5-8] (nuclearity is referred to the metal), with one oxygen to one metal, while the other oxygen interacts weakly with the oxygen of another radical,[9] forming magnetic chains, with the two oxygen atoms to two different metal ions[10,11] (in this case linear chains can be formed, either ferro- or ferrimagnetic, depending on the nature of the metal ion), and with one oxygen atom to two different metal ions, while the second oxygen interacts weakly with the oxygen atom of another radical, thus forming chains of four-spin clusters, which have been called chains of diamonds.[12]

In all these cases the radicals bind to the metal ions, keeping their radical nature; i.e. the spectral and magnetic properties can be best described by considering that the π^* orbital of the nitroxide has a weak overlap with the magnetic orbitals of the metal ions.

Beyond binding to the metal and keeping their radical nature, it is known that nitroxides can undergo redox reactions with transition-metal ions;[13,14] in fact, nitroxyl free radicals are in an oxidation state intermediate between those of the hydroxylamino anion and the nitrosonium cation:

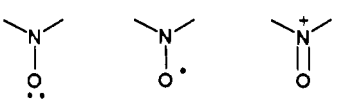

(1) (a) University of Florence. (b) Centre d'Etudes Nucleaires de Grenoble.
(2) Caneschi, A.; Gatteschi, D.; Laugier, J.; Rey, P.; Sessoli, R.; Zanchini, C. In *Organic and Inorganic Low Dimensional Crystalline Materials*; Delhaes, P., Drillon, M., Eds.; Plenum Press: New York, London, 1987; p 381.
(3) Caneschi, A.; Gatteschi, D.; Laugier, J.; Rey, P. In *Organic and Inorganic Low Dimensional Crystalline Materials*; Delhaes, P., Drillon, M., Eds.; Plenum Press: New York, London, 1987; p 109.
(4) Benelli, C.; Caneschi, A.; Gatteschi, D.; Rey, P. In *Organic and Inorganic Low Dimensional Crystalline Materials*; Delhaes, P., Drillon, M., Eds.; Plenum Press: New York, London, 1987; p 385.
(5) Gatteschi, D.; Laugier, J.; Rey, P.; Zanchini, C. *Inorg. Chem.* **1987**, *26*, 938.
(6) Caneschi, A.; Gatteschi, D.; Laugier, J.; Pardi, L.; Rey, P.; Zanchini, C. *Inorg. Chem.* **1988**, *27*, 2027.
(7) Caneschi, A.; Gatteschi, D.; Grand, A.; Laugier, J.; Pardi, L.; Rey, P. *Inorg. Chem.* **1988**, *27*, 1031.
(8) Benelli, C.; Caneschi, A.; Gatteschi, D.; Laugier, J.; Rey, P. *Angew. Chemie.* **1987**, *26*, 913.
(9) Laugier, J.; Rey, P.; Gatteschi, D.; Zanchini, C. *J. Am. Chem. Soc.* **1986**, *108*, 6931.
(10) Caneschi, A.; Gatteschi, D.; Laugier, P.; Rey, P. *J. Am. Chem. Soc.* **1987**, *109*, 2191.
(11) Caneschi, A.; Gatteschi, D.; Rey, P.; Sessoli, R. *Inorg. Chem.* **1988**, *27*, 1756.
(12) Caneschi, A.; Gatteschi, D.; Laugier, J.; Rey, P.; Sessoli, R. *Inorg. Chem.* **1988**, *27*, 1553.
(13) Dickman, M. H.; Doedens, R. J. *Inorg. Chem.* **1982**, *21*, 682.
(14) Porter, L. C.; Doedens, R. J. *Acta Crystallogr.* **1985**, *C41*, 838.

0020-1669/89/1328-1969$01.50/0

Up to now relatively little work has been devoted to the study of the redox properties of metal–nitroxyl systems. The oxidation of a nitroxide by some metal ions in a high oxidation state has been known for a long time, but only two complexes containing metal ions bound to reduced radicals have been reported so far.[13,14] However, such reduced species are expected to be formed when nitroxides react with metal ions in a low oxidation state, such as manganese(II).

The interaction of stable organic radicals with manganese is of particular interest since it is known that manganese can replace iron in the center responsible for photosynthesis in some strains of bacteria, such as *Rhodopseudomonas spheroides*.[15,16] In these native centers, iron(II) interacts with the reduced form of the primary quinone acceptor and also with the semiquinone form of the secondary acceptor.[17,18] Similar results were observed in the manganese-substituted reaction centers. Therefore, it can be anticipated that the study of manganese(II)–nitroxide systems can help to shed light on the kinds of interactions possible for manganese–radical systems in general, their redox properties, and the capacity of manganese for forming polynuclear systems, which are intensively studied at the moment[19-23] in connection with the active site of photosystem II in plant photosynthesis.[24,25]

Manganese(II) hexafluoroacetylacetonate, $Mn(hfac)_2 \cdot 2H_2O$, reacts with NITPh in nonpolar solvents, yielding several different compounds. It can bind as a monodentate ligand, yielding a bis adduct,[6] or as a 1,3-bridging ligand, yielding either a cyclic hexanuclear species[26] or a linear chain.[2] We have now isolated a fourth complex in which the ligand is 1-hydroxy-2-phenyl-4,4,5,5-tetramethyl-4,5-dihydro-1*H*-imidazole (IMHPh), the diamagnetic reduced form of the imino nitroxide 2-phenyl-4,4,5,5-tetramethyl-4,5-dihydro-1*H*-imidazolyl-1-oxy (IMPh), of structure

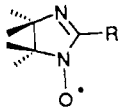

It contains also the starting free radical NITPh, yielding the stoichiometry $[Mn(hfac)_2(IMHPh)]_2(NITPh)$ (I). A somewhat similar behavior was observed by reacting $Mn(hfac)_2 \cdot 2H_2O$ with IMPh, and in this case a compound of formula $Mn(hfac)_2(IMHPh)(IMPh)$ (II) was obtained.

These two compounds are the first examples of derivaties of manganese(II) with a reduced form of a nitroxyl free radical; we wish to report here their synthesis, X-ray crystal structure, and magnetic properties.

Experimental Section

Synthesis of the Complexes. $Mn(hfac)_2 \cdot 2H_2O$ was prepared according to literature methods.[27] The NITPh and IMPh radicals were prepared as previously described.[28-30] Compound I was prepared by adding 2 mmol of NITPh to 50 mL of boiling dry *n*-heptane containing 1 mmol of $Mn(hfac)_2 \cdot 2H_2O$. The solution was refluxed for 2 min and then filtered, and the filtrate allowed to cool down. After 12 h violet crystals suitable for X-ray structure determination were collected. The compound analyzed satisfactorily for $Mn(hfac)_2(IMHPh)_2(NITPh)$. Anal. Calcd for $C_{59}F_{24}H_{57}Mn_2N_6O_{12}$: C, 44.06; H, 3.55; N, 5.23; Mn, 6.85. Found: C, 44.32; H, 3.67; N, 5.18; Mn, 6.71.

Compound II was prepared by adding 1.5 mmol of IMPh radical to a solution of boiling dry *n*-heptane containing 1 mmol of $Mn(hfac)_2 \cdot 2H_2O$ salt, and then the solution was stored for 24 h at 5 °C, and nice orange crystals were obtained. The compound analyzed satisfactorily for $Mn(Hfac)_2(IMHPh)(IMPh)$. Anal. Calcd for $C_{36}F_{12}H_{37}MnN_4O_6$: C, 47.74; H, 4.09; N, 6.19; Mn, 6.08. Found: C, 47.83; H, 4.15; N, 6.12; Mn, 6.0.

X-ray Data Collection and Reduction. X-ray data for $[Mn(hfac)_2(IMHPh)]_2(NITPh)$ (I) and $Mn(hfac)_2(IMHPh)(IMPh)$ (II) were collected on an Enraf-Nonius CAD-4 four-circle diffractometer with Mo Kα radiation. Accurate unit cell parameters were derived from least-squares refinement of the setting angles of 25 reflections and are reported in Table I with other experimental parameters. For both compounds the data were collected from regularly shaped crystals (approximate dimensions listed in Table I); they were corrected for Lorentz and polarization effects but not for adsorption and extintion.

The triclinic crystal symmetry for I and the monoclinic symmetry for II were determined by Weissenberg photographs.

Structure Solution and Refinements. Both crystal structures were solved by conventional Patterson and Fourier methods using the SHELX-76 package.[31] The manganese positions were determined by means of sharpened Patterson functions, and the phase provided by the heavy atoms was used for successive difference syntheses that revealed the positions of the remaining non-hydrogen atoms. Structure refinements were carried out by full-matrix least-squares methods, with anisotropic thermal parameters for all non-hydrogen atoms.

For I the refinement with 4494 reflections $|F_o| > 4\sigma|F_o|$ converged to final R values of $R = 0.067$ and $R_w = 0.069$.

For II the refinement carried out on 3714 reflections with $|F_o| > 4\sigma|F_o|$ and converged to $R = 0.060$ and $R_w = 0.057$. For both compounds the final refinement model included all hydrogen atoms in fixed and idealized positions.

Due to the small size of the crystals, a severe lack of scattered intensity was observed. Accordingly, the data/parameter ratio was low for both the compounds. However, the lack of precision does not hamper the chemical meaning of the structures and no attempt was made to collect more data since we were not able to grow larger crystals.

Atomic positional parameters for I and II are listed in Tables II and III. Selected bond lengths and angles are listed in Tables IV and V.

Magnetic Susceptibility Measurements. Magnetic susceptibilities were measured in the temperature range 300–5 K by using an SHE superconducting SQUID susceptometer at a field strength of 0.5 T. Data were corrected for the magnetization of the sample holder and for diamagnetic contributions, which were estimated from Pascal's constants.

Electron Paramagnetic Resonance Measurements. The polycrystalline powder EPR spectra of $Mn(hfac)_2(IMHPh)(IMPh)$ were recorded with Bruker ER200 and Varian E9 spectrometers operating at X- and Q-band frequencies respectively.

Table I. Summary of Crystal and Data Collection Parameters for $[Mn(hfac)_2(IMHPh)]_2(NITPh)$ (I) and $Mn(hfac)_2(IMHPh)(IMPh)$ (II)

	I	II
chem formula	$C_{59}H_{57}Mn_2O_{12}N_6F_{24}$	$C_{36}H_{37}MnO_7N_4F_{12}$
fw	1607.98	920.63
space group	$P\bar{1}$ (No. 2)	$P2_1/c$ (No. 14)
a, Å	13.566 (2)	13.391 (2)
b, Å	15.079 (3)	22.725 (3)
c, Å	21.622 (4)	14.987 (2)
α, deg	68.36 (2)	90
β, deg	77.18 (2)	66.73 (2)
γ, deg	61.47 (2)	90
V, Å^3	3606.4	4189.7
Z	2	4
d, g cm^{-3}	1.476	1.434
cryst dimens, mm	0.18 × 0.17 × 0.11	0.21 × 0.17 × 0.12
temp, °C	20	20
radiation, Å	0.7107 (Mo Kα)	0.7107 (Mo Kα)
R	0.067	0.060
R_w	0.069	0.057

(15) Feher, G.; Isaacson, R. A.; McElroy, J. D.; Ackerson, L. C.; Okamma, M. Y. *Biochim. Biophys. Acta* **1974**, *368*, 135.
(16) Nam, H. K.; Austin, R. H.; Dismukes, G. C. *Biochim. Biophys. Acta* **1983**, *724*, 340.
(17) Okamma, M. J.; Isaacson, R. A.; Feher, G. *Proc. Natl. Acad. Sci.* **1975**, *72*, 3491.
(18) Wraight, C. A. *Biochim. Biophys. Acta* **1977**, *459*, 525.
(19) Mabad, B.; Cassoux, P.; Tuchagues, J. P.; Hendrickson, D. N. *Inorg. Chem.* **1986**, *25*, 1420.
(20) Morrison, M. M.; Sawyer, D. T. *J. Am. Chem. Soc.* **1977**, *99*, 257.
(21) Cooper, S. T.; Calvin, M. *J. Am. Chem. Soc.* **1977**, *99*, 6623.
(22) Cooper, S. R.; Dismukes, G. C.; Klein, M. P.; Calvin, M. *J. Am. Chem. Soc.* **1978**, *100*, 7428.
(23) Mathur, P.; Dismukes, G. C. *J. Am. Chem. Soc.* **1983**, *105*, 7093.
(24) Saner, K. *Acc. Chem. Res.* **1980**, *13*, 249.
(25) de Paula, J. C.; Brudvig, G. W. *J. Am. Chem. Soc.*, **1986**, *108*, 4002.
(26) Caneschi, A.; Gatteschi, D.; Laugier, P.; Rey, P.; Sessoli, R.; Zanchini, C. *J. Am. Chem. Soc.* **1988**, *110*, 2795.
(27) Cotton, F. A.; Holm, R. H. *J. Am. Chem. Soc.* **1960**, *82*, 2979.
(28) Shechter, H.; Kaplan, R. B. *J. Am. Chem. Soc.* **1953**, *75*, 3980.
(29) Lamchen, M.; Wittag, T. W. *J. Chem. Soc. C* **1966**, 2300.
(30) Ullman, E. F.; Call, L.; Osiecky, J. H. *J. Org. Chem.* **1970**, *35*, 3623.
(31) (a) Sheldrick, G. "SHELX 76 System of Computing Programs"; University of Cambridge: Cambridge, England (b) Busing, W. R.; Martin, K. O.; Levy, H. A. *Oak Ridge Natl. Lab. [Rep.], ORNL (U.S.)* **1971**, *ORNL-594.32*.

Table II. Atomic Positional Parameters for I[a]

	x	y	z	B_{eq}, Å^2		x	y	z	B_{eq}, Å^2
Mn1	5260 (1)	3721 (1)	5071 (1)	5.06	C29	3106 (9)	3101 (10)	2022 (6)	10.28
O1	6821 (5)	2383 (5)	4915 (3)	6.23	C30	2102 (11)	2221 (9)	1739 (6)	11.04
O2	5053 (5)	3863 (5)	4069 (3)	6.34	C31	−149 (11)	5238 (9)	2669 (6)	8.79
O3	4283 (6)	2823 (6)	5317 (4)	7.25	C32	186 (17)	5670 (13)	3006 (9)	17.72
O4	5597 (5)	2883 (5)	6119 (3)	6.10	C33	−538 (26)	6686 (17)	3007 (11)	23.88
O5	6058 (5)	4731 (4)	4922 (3)	4.93	C34	−1611 (26)	7176 (17)	2776 (11)	21.19
N1	7225 (6)	4319 (5)	4851 (4)	5.08	C35	−1942 (15)	6787 (12)	2367 (10)	15.40
N2	8930 (7)	3558 (7)	4450 (5)	7.78	C36	−1156 (11)	5726 (10)	2342 (7)	11.35
C1	6922 (9)	1841 (8)	4554 (6)	6.30	Mn2	−1216 (1)	683 (1)	10425 (1)	5.32
C2	6302 (10)	2092 (9)	4037 (6)	7.01	O8	−2016 (6)	2290 (5)	10460 (3)	6.98
C3	5410 (10)	3108 (10)	3855 (6)	6.75	O9	−2540 (6)	1373 (5)	9749 (3)	7.15
C4	7941 (16)	750 (13)	4713 (10)	10.71	O10	−615 (6)	368 (5)	11384 (4)	6.81
C5	4788 (16)	3274 (18)	3281 (10)	11.42	O11	−2430 (7)	242 (6)	11121 (4)	8.57
C6	4450 (10)	1950 (10)	5776 (7)	7.08	O12	237 (4)	794 (4)	9824 (3)	4.82
C7	5064 (10)	1490 (9)	6330 (6)	6.98	N5	397 (7)	1690 (6)	9650 (4)	5.43
C8	5588 (9)	2004 (9)	6449 (6)	6.14	N6	141 (8)	3319 (6)	9224 (5)	8.07
C9	3953 (21)	1306 (21)	5649 (11)	11.83	C37	−3065 (13)	2879 (8)	10404 (6)	8.33
C10	6210 (18)	1471 (13)	7063 (8)	9.46	C38	−3834 (11)	2881 (10)	10083 (7)	9.10
C11	7831 (9)	4078 (8)	4322 (6)	5.92	C39	−3466 (11)	2127 (11)	9772 (7)	7.67
C12	7912 (8)	4114 (9)	5392 (6)	6.27	C40	−3446 (17)	3731 (14)	10743 (11)	12.65
C13	9051 (9)	3348 (10)	5164 (6)	8.09	C41	−4349 (19)	2206 (16)	9444 (15)	14.81
C14	7432 (9)	3742 (10)	6064 (6)	8.91	C42	−1181 (15)	448 (8)	11925 (7)	8.02
C15	9182 (12)	2144 (11)	5515 (8)	11.97	C43	−2228 (15)	452 (11)	12106 (8)	9.97
C16	10096 (9)	3374 (12)	5259 (7)	12.81	C44	−2731 (13)	349 (10)	11678 (9)	9.44
C17	7942 (9)	5182 (9)	5278 (7)	9.48	C46	−3912 (22)	369 (14)	11872 (12)	16.45
C18	7422 (9)	4324 (9)	3677 (5)	6.32	C47	−176 (9)	2586 (9)	9227 (5)	6.14
C19	6504 (9)	5293 (8)	3401 (6)	6.97	C48	777 (12)	2950 (9)	9819 (8)	8.77
C20	6205 (10)	5491 (10)	2777 (7)	8.44	C49	1304 (10)	1721 (8)	9940 (6)	6.61
C21	6773 (12)	4748 (12)	2424 (7)	9.97	C50	−102 (11)	3336 (10)	10367 (7)	12.10
C22	7657 (12)	3781 (12)	2706 (7)	9.69	C51	1634 (12)	3406 (9)	9639 (8)	10.97
C23	8020 (9)	3538 (9)	3346 (6)	7.85	C52	2409 (9)	1282 (9)	9534 (7)	11.11
F1	8130 (9)	326 (7)	5338 (6)	17.05	C53	1387 (11)	1078 (9)	10676 (7)	8.91
F2	8857 (9)	816 (7)	4456 (6)	16.52	C54	−1024 (10)	2809 (8)	8806 (5)	6.29
F3	7897 (9)	75 (7)	4515 (7)	19.19	C55	9152 (11)	2100 (9)	8487 (6)	8.26
F4	3741 (9)	3542 (12)	3425 (6)	18.10	C56	7205 (11)	4029 (9)	8312 (7)	9.14
F5	5196 (9)	2647 (9)	2970 (6)	20.38	C57	8023 (11)	3783 (8)	8716 (5)	7.17
F6	4641 (12)	4196 (11)	2830 (6)	16.50	C58	7357 (13)	3366 (12)	7970 (7)	10.63
F7	3775 (18)	1505 (14)	5091 (6)	21.28	C59	8324 (15)	2396 (12)	8063 (7)	10.94
F8	2895 (11)	1663 (14)	5901 (11)	26.21	F13	−4537 (8)	4220 (9)	10827 (6)	20.33
F9	4270 (13)	396 (9)	5958 (9)	18.32	F14	−3006 (12)	3494 (9)	11246 (6)	22.06
F10	7291 (11)	1198 (10)	6929 (6)	16.90	F15	−3207 (13)	4521 (9)	10316 (8)	21.25
F11	5930 (15)	1982 (8)	7429 (6)	23.59	F16	−4056 (10)	1683 (14)	9038 (8)	22.07
F12	6278 (8)	535 (7)	7418 (4)	12.23	F17	−5068 (13)	3093 (10)	9124 (10)	22.60
O6	794 (6)	4458 (6)	1460 (4)	8.86	F18	−4980 (14)	1815 (18)	9837 (8)	24.07
O7	964 (7)	3282 (7)	3709 (5)	12.03	F22	−4330 (8)	531 (9)	12436 (5)	19.47
N3	1082 (8)	3857 (7)	2062 (6)	7.54	F23	−4660 (8)	1035 (12)	11476 (6)	19.52
N4	1136 (9)	3316 (9)	3103 (6)	8.70	F24	−3840 (8)	−556 (10)	11978 (7)	22.11
C24	665 (9)	4164 (9)	2610 (7)	6.96	C45	−579 (29)	524 (21)	12370 (11)	16.81
C25	1840 (9)	2322 (8)	2937 (7)	7.53	F19	262 (14)	−168 (13)	12566 (9)	31.05
C26	2075 (10)	2799 (8)	2196 (6)	7.10	F20	−468 (18)	1364 (18)	12191 (9)	25.69
C27	2903 (10)	1659 (9)	3347 (7)	9.98	F21	−1217 (13)	796 (16)	12886 (7)	26.95
C28	1112 (9)	1727 (8)	3090 (7)	10.00					

[a] Coordinates are multiplied by 10^4. Standard deviations in the last significant digits are in parentheses.

Results

Synthesis. The chemistry of the system $Mn(hfac)_2$ + NITPh has proved to be an extremely rich one. At least four different well characterized crystalline derivatives can be obtained according to the experimental conditions. Sometimes we have been able to obtain mainly one species, but more often mixtures of various compounds are formed. However, the following lines seem to be well established.

If the $Mn(hfac)_2$:(NITPh) ratio is 1:1, or slightly larger, and the solution in *n*-heptane is warmed to ca. 80 °C, the main product is $[Mn(hfac)_2(NITPh)]_6$, a cyclic hexanuclear species.[26] With the same stoichiometric ratio, but with operation at lower temperature, a polymeric $Mn(hfac)_2(NITPh)$ compound is isolated.[11] Magnetic measurements indicate a chain structure, but up to now we were not able to obtain single crystals suitable for X-ray determination.

If the $Mn(hfac)_2$:(NITPh) ratio is 1:2 and the solution in *n*-heptane is warmed to a maximum of 70 °C, then a mononuclear bis adduct is obtained.[6] On the other hand, if the solution is allowed to reach the ebullition temperature, compound I is obtained. NITPh is reduced to IMHPh, and the reduced *N*-oxide derivative thus obtained binds to the manganese ions, as shown below by the crystal structure determination.

The deoxygenation of nitronyl nitroxides into imino nitroxides has been reported to occur under a variety of conditions,[30-32] most of which were not predicted to lead this new class of free radicals. In any case, it has been established that active acid derivatives were able to perform this deoxygenation step. Although the mechanistic details of the reaction are uncertain, and the product derived from $Mn(hfac)_2$ is not yet characterized, it is now established that $Mn(hfac)_2$ is able to convert NITPh into IMPh. However, the reducing process does not stop at this stage, because the isolated complex contains IMHPh, the reduced form of IMPh. Since the starting nitroxide (NITPh) is also present in $[Mn(hfac)_2(IMHPh)]_2(NITPh)$, it must be concluded that the second reducing step is favored; i.e., the one-electron reduction of IMPh into IMHPh is easier than the deoxygenation step of NITPh into

(32) Ullman, E. F.; Osiecki, J. K.; Boccock, D. G. B.; Darcy, R. *J. Am. Chem. Soc.* **1972**, *74*, 7049.

Table III. Atomic Positional Parameters for II[a]

	x	y	z	B_{eq}, Å^2
Mn	4745 (1)	5330 (0)	4073 (1)	4.39
F1	2058 (9)	6001 (5)	3078 (10)	26.61
F2	1439 (6)	6373 (6)	4320 (7)	22.37
F3	2221 (7)	6857 (4)	3181 (10)	29.92
F4	5411 (6)	7657 (3)	3401 (8)	21.38
F5	6399 (8)	7141 (4)	2400 (5)	19.86
F6	6461 (6)	7202 (3)	3684 (7)	21.48
F7	3140 (7)	3687 (3)	2902 (9)	23.16
F8	2839 (8)	4212 (5)	1995 (5)	27.25
F9	2091 (6)	4295 (4)	3402 (7)	16.80
F10	5720 (7)	5436 (4)	215 (4)	20.57
F11	5812 (6)	6154 (3)	1004 (5)	15.04
F12	6972 (6)	5533 (4)	620 (4)	14.92
O1	3319 (3)	5782 (2)	4107 (3)	6.10
O2	5319 (3)	6232 (2)	3984 (3)	5.62
O3	5678 (3)	5379 (2)	2517 (3)	6.03
O4	4012 (3)	4608 (2)	3550 (3)	5.44
O5	5990 (3)	4893 (2)	4403 (3)	3.93
O6	10251 (7)	2588 (4)	−635 (5)	14.49
N1	7014 (4)	4734 (2)	3750 (3)	4.11
N2	8422 (4)	4165 (2)	2998 (4)	4.97
N3	9495 (4)	3193 (2)	1614 (4)	5.78
N4	10203 (6)	2753 (3)	179 (5)	7.92
C1	3310 (6)	6269 (3)	3715 (5)	6.06
C2	4092 (6)	6701 (3)	3437 (6)	7.23
C3	5033 (6)	6646 (3)	3601 (5)	5.49
C4	2274 (10)	6363 (6)	3558 (12)	12.84
C5	5842 (8)	7144 (4)	3259 (9)	8.74
C6	3888 (5)	4613 (3)	2773 (5)	5.52
C7	4467 (6)	4926 (3)	1933 (5)	6.62
C8	5326 (6)	5276 (3)	1874 (5)	5.93
C9	2974 (10)	4226 (5)	2739 (8)	9.01
C10	5922 (9)	5608 (5)	932 (7)	8.77
C11	7347 (5)	4191 (3)	3524 (4)	4.26
C12	7958 (5)	5151 (3)	3482 (5)	4.96
C13	8820 (5)	4771 (3)	2674 (5)	5.63
C14	8761 (7)	4866 (4)	1672 (6)	7.75
C15	9978 (6)	4859 (4)	2570 (7)	8.00
C16	8226 (6)	5219 (3)	4377 (5)	7.15
C17	7716 (6)	5739 (3)	3158 (6)	7.22
C18	6696 (5)	3650 (3)	3761 (4)	4.45
C19	5664 (5)	3635 (3)	3735 (5)	5.55
C20	5143 (7)	3108 (4)	3854 (6)	7.16
C21	5615 (8)	2590 (4)	4025 (6)	7.98
C22	6619 (8)	2612 (3)	4071 (6)	7.72
C23	7170 (6)	3137 (3)	3935 (5)	6.29
C24	9391 (5)	3119 (3)	810 (5)	5.58
C25	11051 (6)	2635 (4)	559 (6)	7.86
C26	10418 (5)	2820 (3)	1627 (5)	6.10
C27	11974 (7)	3053 (6)	25 (8)	15.42
C28	11411 (9)	2007 (4)	361 (7)	13.46
C29	11042 (6)	3165 (4)	2100 (7)	11.01
C30	9911 (6)	2288 (3)	2284 (6)	9.15
C31	8533 (6)	3374 (3)	556 (5)	6.42
C32	7471 (6)	3379 (3)	1240 (6)	7.36
C33	6663 (7)	3646 (4)	1035 (7)	9.31
C34	6916 (9)	3901 (4)	136 (9)	11.61
C35	7997 (10)	3898 (4)	−563 (8)	12.63
C36	8791 (8)	3634 (4)	−356 (6)	9.40

[a] Coordinates are multiplied by 10^4. Standard deviations in the last significant digits are in parentheses.

IMPh. Further support for this hierarchy in the reducing steps comes from the reaction of the preformed IMPh with $Mn(hfac)_2$, which shows that the formation of IMHPh is independent of NITPh.

The resulting reduced species (IMHPh) can exist in principle in two tautomeric forms,[30-32] i.e. either as amidino oxide or imino hydroxylamine, and the phenyl derivative (IMHPh) has been reported to exist predominantly in the amidino oxide form. The complete redox process is shown in Figure 1. This seems also to be the case in the two complexes I and II, as shown by X-ray diffraction study (vide infra).

Crystal Structure. The crystal structure of I consists of two different centrosymmetric units, of formulas $[Mn(hfac)_2$-$(IMHPh)(NITPh)]_2$ and $[Mn(hfac)_2(IMHPh)]_2$, respectively. In the latter moiety two manganese(II) ions are bridged by two oxygen atoms of two IMHPh molecules. Each manganese is hexacoordinated to two hexafluoroacetylacetonate ligands and to two oxygen atoms of two different IMHPh molecules. The latter two atoms occupy two cis positions in the coordination octahedron. All the Mn–O bond distances are rather similar to each other and in the normal range for this kind of compound. A view of $[Mn(hfac)_2(IMHph)]_2$ is shown in Figure 2. The N–O bond distance in IMHPh is clearly indicative of the reduced form of the radical, since it is 1.392 (9) Å, while the corresponding distance in nitroxides[33-37] nitronyl nitroxides[6-12] ranges from 1.25 to 1.32

Table IV. Selected Bond Distances (Å) for $[Mn(hfac)_2(IMHPh)]_2(NITPh)$ (I) and $Mn(hfac)_2(IMHPh)(IMPh)$ (II)

		I			
Mn1–O1	2.185 (5)	Mn1–O2	2.165 (7)	Mn1–O3	2.178 (10)
Mn1–O4	2.176 (6)	Mn1–O5	2.157 (8)	Mn1–O5′	2.165 (8)
Mn1–Mn1′	3.474 (7)	N1–O5	1.392 (9)	Mn2–O8	2.155 (7)
Mn2–O9	2.169 (7)	Mn2–O10	2.201 (9)	Mn2–O11	2.151 (8)
Mn2–O12	2.151 (5)	Mn2–O12′	2.160 (8)	Mn2–Mn2	3.476 (8)
		II			
Mn1–O1	2.151 (4)	Mn1–O2	2.175 (4)	Mn2–O3	2.170 (4)
Mn1–O4	2.209 (4)	Mn1–O5	2.159 (4)	Mn1–O5′	2.159 (3)
Mn1–Mn1′	3.455 (6)	N1–O5	1.381 (5)	N4–O6	1.255 (11)

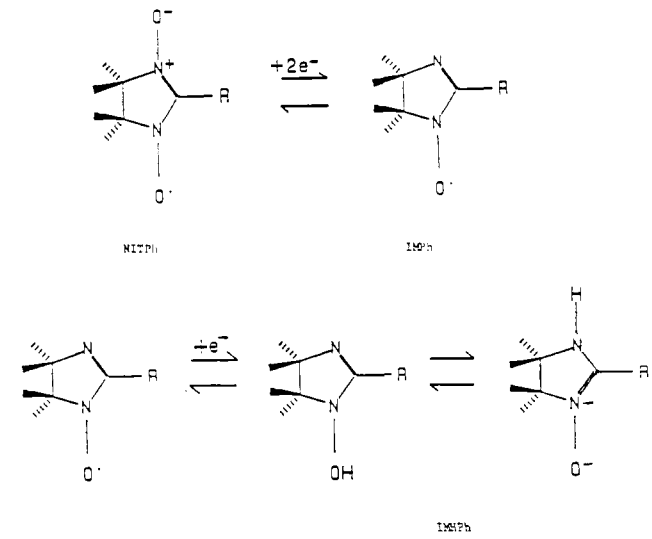

Figure 1. Scheme of the redox process for the NITPh radicals.

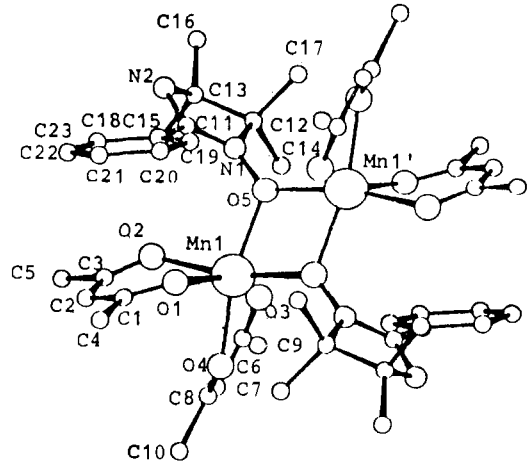

Figure 2. ORTEP view of the $[Mn(hfac)_2(IMHPh)]_2$ unit.

(33) Dickman, M. H.; Porter, L. C.; Doedens, R. J. *Inorg. Chem.* **1986**, *25*, 2595.
(34) Anderson, O. P.; Kuechler, T. C. *Inorg. Chem.* **1980**, *19*, 1417.
(35) Grand, A.; Rey, P.; Subra, R. *Inorg. Chem.* **1983**, *22*, 391.

Table V. Selected Angles (deg) for $[Mn(hfac)_2(IMHPh)]_2(NITPh)$ (I) and $Mn(hfac)_2(IMHPh)(IMPh)$ (II)

			I		
O1–Mn1–O2	80.5 (2)	O1–Mn1–O3	92.7 (2)	O1–Mn1–O4	83.5 (2)
O1–Mn1–O5	94.3 (2)	O2–Mn1–O3	81.4 (3)	O2–Mn1–O4	154.8 (3)
O2–Mn1–O5	103.8 (2)	O3–Mn1–O4	80.0 (3)	O3–Mn1–O5	171.8 (2)
O4–Mn1–O5	96.7 (3)	O5–Mn1–O5′	72.7 (2)	Mn1–O5–N1	119.6 (3)
Mn1–O5–Mn1′	107.3 (2)	O8–Mn2–O9	80.3 (3)	O8–Mn2–O10	81.9 (2)
O8–Mn2–O11	94.11 (3)	O8–Mn2–O12	95.5 (2)	O9–Mn2–O10	152.0 (2)
O9–Mn2–O11	81.5 (3)	O9–Mn2–O12	96.9 (2)	O10–Mn2–O11	78.4 (3)
O10–Mn2–O12	96.3 (2)	O11–Mn2–O12	68.2 (2)	O12–Mn2–O12′	73.0 (3)
Mn2–O11–N3	121.4 (4)	Mn2–O12–Mn2	107.0 (2)		
			II		
O1–Mn1–O2	80.8 (1)	O1–Mn1–O3	97.5 (1)	O1–Mn1–O4	81.3 (1)
O1–Mn1–O5	166.6 (1)	O2–Mn1–O3	81.2 (1)	O2–Mn1–O4	150.0 (1)
O2–Mn1–O5	99.3 (1)	O3–Mn1–O4	78.7 (1)	O3–Mn1–O5	95.8 (1)
O4–Mn1–O5	103.4 (1)	O5–Mn1–O5′	73.8 (1)	Mn1–O5–N1	126.7 (1)

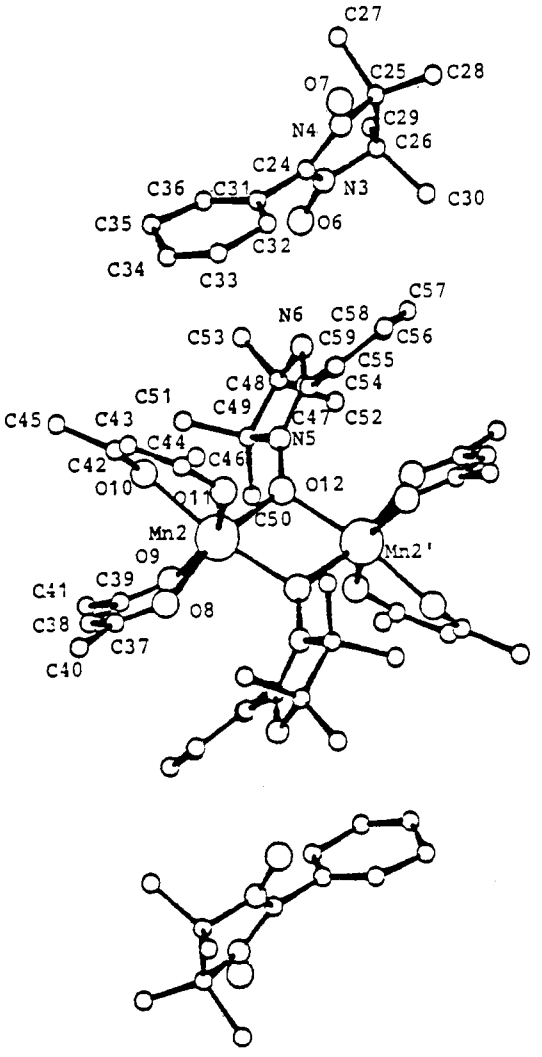

Figure 3. ORTEP view of the $[Mn(hfac)_2(IMHPh)(NITPh)]_2$ unit.

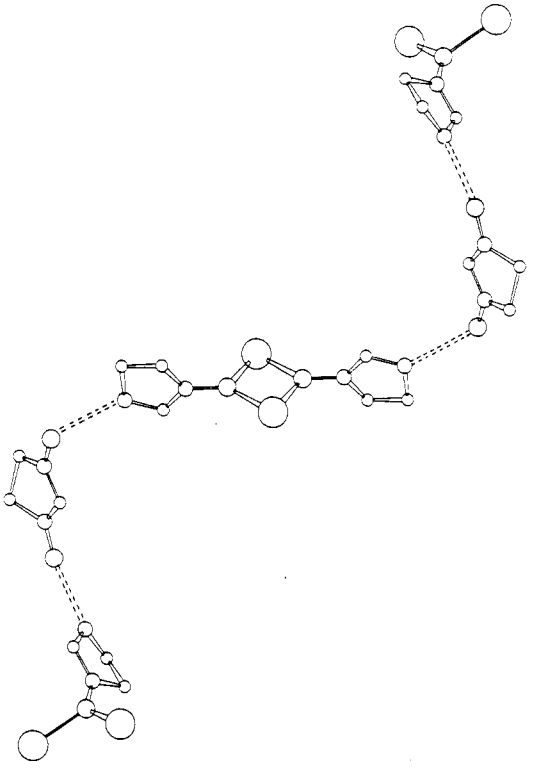

Figure 4. Sketch of the chain formed by $[Mn(hfac)_2(IMHPh)(NITPh)]$ units.

Å. As mentioned above, the reduced radical can exist in two tautomeric form, the *N*-oxide and the hydroxylamino ones. Since the oxygen atom is here involved in bonding to two different metal ions, it is the former that seems to be more probable. The imidazoline ring is planar, and the angle of this plane with that of the phenyl group is 36.5 (4)°.

The other unit $[Mn(hfac)_2(IMHPh)(NITPh)]_2$ can be described as the adduct of $[Mn(hfac)_2(IMHPh)]_2$ with two NITPh radicals, as shown in Figure 3. The $[Mn(hfac)_2(IMHPh)]_2$ moiety is very similar to the analogous one of the other unit. In particular the N–O bond distance of 1.372 (12) Å is strongly indicative of the reduced form of the radical that is bound to manganese. The NITPh solvate molecule is located between the two dimers in such a way that its oxygen atoms are close to the imino nitrogens of the bridging IMHPh. These contacts of 2.82 (2) and 2.76 (2) Å are clearly indicative of hydrogen bonding.[38] Therefore, compound I is organized in chains, as sketched on Figure 4. The bond distances within the NITPh radical are as expected. In particular, the N–O distances are 1.26 (2) and 1.30 (1) Å, much shorter than in the reduced forms. The ring of the nitroxide is planar, and the angle with the phenyl group is 39.9 (4)°.

The crystal structure of II consists of centrosymmetric units $[Mn(hfac)_2(IMHPh)(IMPh)]_2$, as shown in Figure 5. The $[Mn(hfac)_2(IMHPh)]_2$ moiety is very similar to the analogous ones in I, again characterized by a long N–O bond of 1.381 (5) Å. The amidino nitrogen has a short contact with the analogous atom of the radical IMPh, 2.983 (7) Å, suggesting a hydrogen-bonding interaction. The free-radical nature of this solvate molecule is reflected in the short N–O bond distance of 1.255 (9) Å.

(36) Laugier, J.; Ramasseul, R.; Rey, P.; Espie, J. C.; Rassat, A. *Nouv. J. Chim.* **1983**, *7*, 11.
(37) Dickmann, M. H.; Porter, L. C. *Inorg. Chem.* **1986**, *25*, 3453.
(38) Pauling, L. *The Nature of the Chemical Bond*, 3rd ed.; Cornell University Press: Ithica, NY, 1960; p 260.

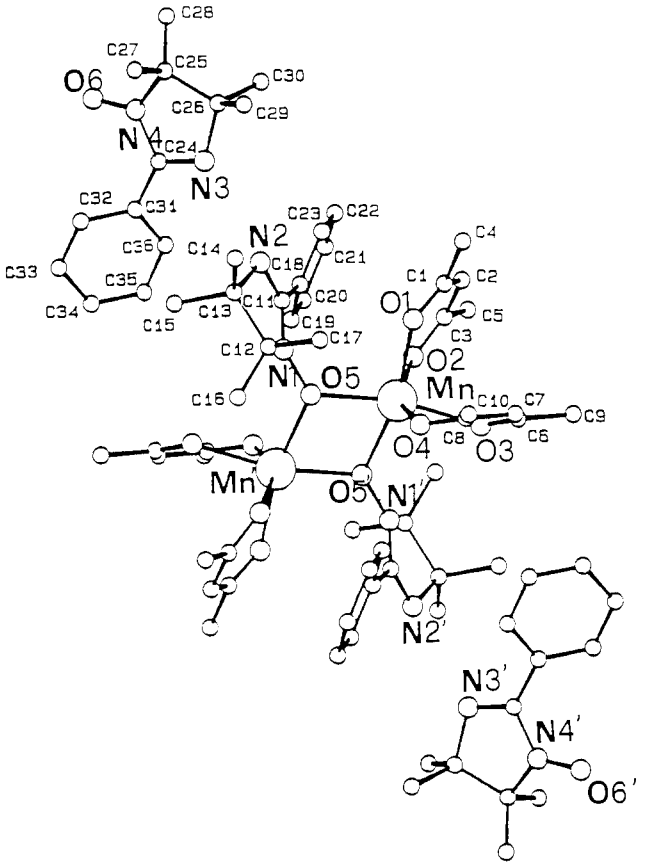

Figure 5. ORTEP view of the $[Mn(hfac)_2(IMHPh)(IMPh)]_2$ unit.

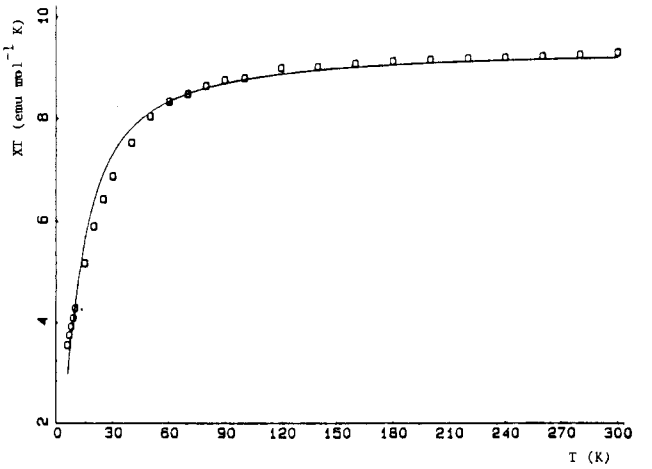

Figure 6. χT vs T dependence in the range 6–300 K for I. The curve is calculated as described in the text.

Magnetic Measurements. The temperature dependence of χT for I in the range 6–300 K is shown in Figure 6. The molar susceptibility is calculated for the formula unit $[Mn(hfac)_2(IMHPh)]_2(NITPh)$. The χT value decreases steadily from 8.89 emu mol^{-1} K at room temperature to 3.31 emu mol^{-1} K at 6 K. The room-temperature value compares well with that of 9.125 emu mol^{-1} K expected for two $S = {}^5/_2$ and one $S = {}^1/_2$ uncoupled spins corresponding to two manganese(II) and one radical. It is apparent that an antiferromagnetic coupling is operative between the spins; however, the χ vs T curve does not show any maximum.

The temperature dependence of χT for II in the range 5–300 K is shown in Figure 7. The molar susceptibility is calculated for the formula unit $[Mn(hfac)_2(IMHPh)(IMPh)]_2$. Also in this case χT decreases on decreasing temperature. The room-temperature value, 9.248 emu mol^{-1} K, is slightly lower than that expected for two $S = {}^5/_2$ and two $S = {}^1/_2$ uncorrelated spins (9.5 emu mol^{-1} K), while the small low-temperature value 1.877 emu

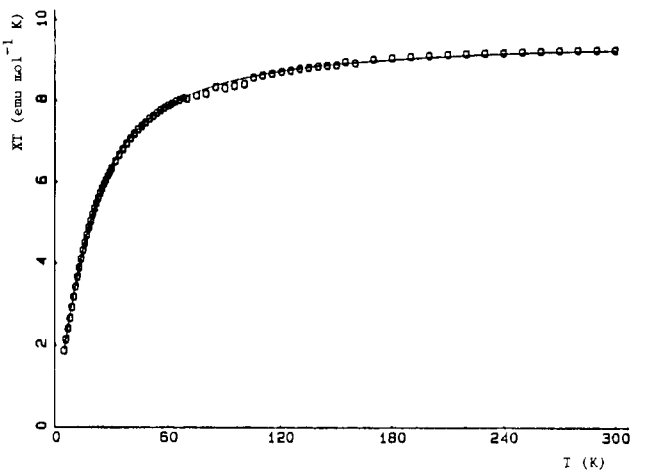

Figure 7. χT vs T dependence in the range 5–300 K for II. The curve is calculated as described in the text.

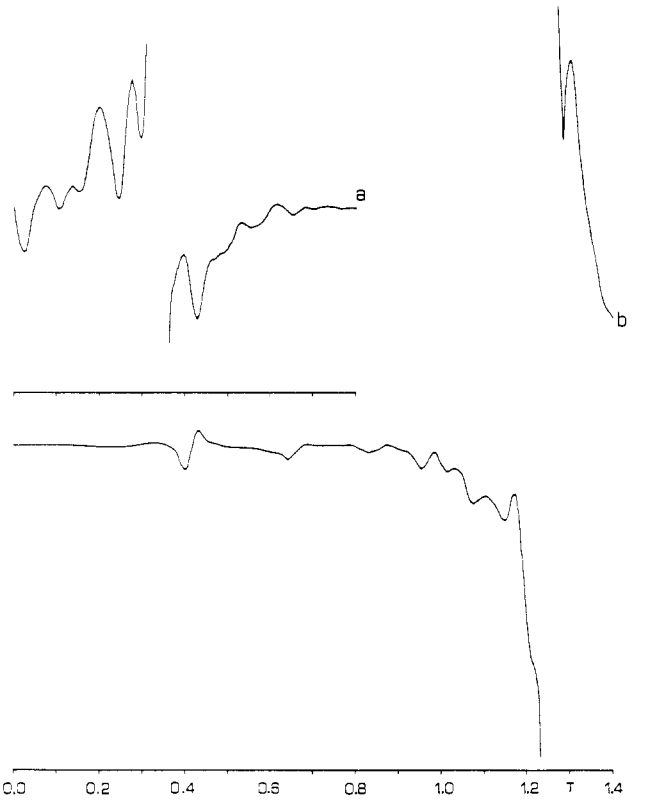

Figure 8. EPR polycrystalline powder spectra of $Mn(hfac)_2(IMHPh)(IMPh)$ recorded at room temperature at X- (a) and Q-band (b) frequencies.

mol^{-1} K also is indicative of a predominant antiferromagnetic interaction, and the χ vs T curves does not show any maximum.

EPR Spectra. The polycrystalline powder EPR spectrum of I shows a broad feature at $g = 2$ and an additional one at $g = 3$. The spectra are practically frequency and temperature independent. The polycrystalline powder EPR spectra of II recorded at room temperature at both X- and Q-band frequencies are shown in Figure 8. They show a relatively sharp feature at $g = 2$, with many additional transitions ranging from 0 to 0.7 T at X-band frequency and from 0.4 to the highest field of our apparatus, 1.4 T, at Q-band frequency. The spectra are practically independent of temperature down to 4.2 K.

Discussion

The magnetic properties of compounds I and II are consistent with dinuclear manganese(II) species, bridged by an amidino oxide diamagnetic ligand. We will first discuss the properties of II, where only one type of magnetic species is present in the unit cell.

From the magnetic point of view II may be schematized as

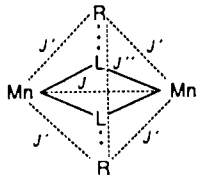

where L stands for IMHPh, and R for NITPh.

Since the NITPh radicals are hydrogen bonded to the amidino oxide ligands, they might interact via superexchange with the manganese ions. They also may interact via superexchange, but since they are fairly distant from each other, this does not seem to be a very probable exchange pathway. From a qualitative analysis of the χT curve we may say that the magnetic properties are dominated by the value of J. In fact, if J' were important, the system should behave like a ring of four spins, yielding either a $S = 6$ or $S = 4$ ground state, for ferro- and antiferromagnetic coupling, respectively.[39] Since the χT value at low temperature is much lower than either limit, we attempted a fit using only J, neglecting J and J'', *i.e.* using a molar susceptibility given by $\chi = \chi(\text{pair}) + 0.750/T$. The calculated curve obtained with $J = 2.88$ cm^{-1} and $g = 2.007$ is shown in Figure 7, and the agreement can be considered as very good. We use the spin Hamiltonian in the form $H = JS_1 \cdot S_2$. From the experimental χ we can easily obtain the values of χ(pair). The χ(pair) vs T plot shows a maximum around 12 K as expected for the reported value of J. Therefore, we did not attempt to include other parameters, such as the other coupling constants, or single-ion zero-field splitting for manganese(II).

The same model was used for I, without taking into account the complications of two different molecules in the cell; i.e., for the formula unit $[Mn(hfac)_2(IMHPh)]_2(NITPh)$, one coupling constant, J, between two manganese ions was included and the radical spin was considered to be not interacting. The best fit values are $J = 1.75$ cm^{-1} and $g = 2.02$. The calculated curve is shown in Figure 6. The calculated parameters compare well with those of II, although the overall agreement with the experimental data is less satisfactory. As a result of the complexity of the structure, we did not include any other sophistication in the fit. We tried also to fit the magnetic data of I and II in the assumption that the bridging ligands are radicals, rather than reduced species, but no agreement with the experimental data could be found, confirming our interpretation of the structure of these Mn complexes.

The observed coupling constants can be justified on an orbital model. The manganese(II) orbitals mostly involved in the superexchange interaction are the $x^2 - y^2$,[7] with the reference frame chosen with the z axis orthogonal to the Mn_2O_2 bridge plane. Since the Mn–O–Mn angles are larger then 106°, the pathway involving the metal $x^2 - y^2$ is an efficient one to yield strong antiferromagnetic coupling, as shown by μ-pyridine N-oxide complexes of copper(II).[40,41] For this last class of compounds, J values larger than 500 cm^{-1} have been reported. If we assume that one pathway is operative for both copper and manganese, the two coupling constants should be[42] in the ratio 1:25 (manganese to copper). In general this simple rule overestimates the coupling constants of manganese, possible reasons being the presence of additional ferromagnetic pathways between the other magnetic orbitals on manganese and the less covalent metal–ligand interactions in manganese(II) compared to those in copper(II).

Crystal structures are available only for few oxo-bridged manganese(II) dimers, so direct comparison with other complexes of this kind is extremely difficult. A coupling constant $J = 1.88$ (6) cm^{-1} has been reported for a Schiff base manganese(II) dimer,[43] and $J = 5.0$ cm^{-1} for a bis(μ-aryloxy)-bridged manganese pair.[44] A Schiff base manganese(II) dimer,[19] for which the crystal structure is not available, shows a $J = 1.30$ cm^{-1}.

The EPR spectra of I, and especially of II, are in agreement with this interpretation. In fact, the spectra of the latter show more details, so that an interpretation can be attempted with some confidence, even in the absence of single-crystal work, which we intend to perform when suitable crystals will be available. First of all, for both complexes the number of unpaired electrons is even, so that in the presence of even a moderate zero-field splitting no transitions should be observed at $g = 2$. However, since this is observed for both complexes, we may conclude that the radicals are essentially uncoupled and resonate at the free-electron value. On this basis the other features should be assigned to the $S = 5$, 4, 3, 2, and 1 total spin states. At Q-band frequency beyond the central line there are five features at lower fields and two at higher fields separated by approximately 60 mT. A similar trend is also observed at X-band frequency, even if with less regularity. We assign this pattern to the perpendicular transition within the $S = 5$ state, with a zero-field splitting of 60 mT, in the assumption that the spectra correspond to the limit of zero-field splitting much smaller than the Zeeman energy at Q-band frequency. Since the observed zero-field splitting has both a dipolar and a single-ion component, it is not possible to discuss this value further, except to say that it is of the same order of magnitude of the dipolar component. Similar values were previously reported for manganese(II) dimers[45] and for cadmium-doped TMMC.[46]

Acknowledgment. The financial support of the CNR and of the Ministry of Public Education is gratefully acknowledged.

Registry No. I, 119681-31-1; II, 119681-32-2; NITPh, 18390-00-6; IMPh, 26731-64-6; $Mn(hfac)_2$, 19648-86-3.

Supplementary Material Available: Tables SI–SIII, listing complete crystallographic data and experimental parameters, complete bond lengths and angles, and anisotropic thermal parameters (23 pages); Table SIV, listing observed and calculated structure factors (39 pages). Ordering information is given on any current masthead page.

(39) Kahn, O. In *Organic and Inorganic Low Dimensional Crystalline Materials*; Delhaes, P., Drillon, M., Eds.; Plenum Press: New York, London, 1987; p 93.

(40) Kokoszka, G. F.; Allen, H. C., Jr.; Gordon, G. *J. Chem. Phys.* **1967**, *46*, 3013.

(41) Estes, E. D.; Hodgson, D. J. *Inorg. Chem.* **1976**, *15*, 348.

(42) Eremin, M. V.; Rakitin, Yu. V. *Phys. Status Solidi* **1977**, *B80*, 579.

(43) Kessissoglou, D. P.; Butler, W. M.; Pecoraro, V. L. *Inorg. Chem.* **1987**, *26*, 495.

(44) Coucouvanis, D.; Greiwe, K.; Salifoglou, A.; Challen, P.; Simopoulos, A.; Kostikas, A. *Inorg. Chem.* **1988**, *27*, 594.

(45) Mathur, P.; Crowder, M.; Dismukes, G. C. *J. Am. Chem. Soc.* **1987**, *109*, 5227.

(46) Clement, S.; Renard, J. P. *J. Magn. Reson.* **1984**, *60*, 46.